THE JOURNAL OF PHYSICAL CHEMISTRY A

Article

pubs.acs.org/JPCA

Structure of the Submonolayer of Ethanol Adsorption on a Vapor/Fused Silica Interface Studied with Sum Frequency Vibrational Spectroscopy

Huijie Xu,[†] Donghua Zhang,[‡] Jun Hu,[‡] Chuanshan Tian,*[,†,§] and Y. Ron Shen*[,†,∥]

[†]Department of Physics, State Key Laboratory of Surface Physics, and Key Laboratory of Micro- and Nano-Photonic Structures (MOE), Fudan University, Shanghai 200433, China

[‡]Key Laboratory of Interfacial Physics and Technology, Shanghai Institute of Applied Physics, Chinese Academy of Sciences, Shanghai 201800, China

[§]Collaborative Innovation Center of Advanced Microstructures, Nanjing 210093, China

[∥]Department of Physics, University of California, Berkeley, California 94720, United States

Supporting Information

ABSTRACT: Sum-frequency vibrational spectroscopy in the CH and OH stretch region was used to study ethanol adsorption on fused silica from vapor of different ethanol partial pressures. It was found that the adsorbed ethanol molecules were oriented with their methyl group tilted away from the surface normal by an average angle of ~45° at low ethanol vapor pressures and ~39° when approaching saturated vapor pressure. The spectral change with ethanol vapor pressure and the deduced adsorption isotherm show that ethanol molecules have two distinct adsorption sites on silica: One is the silanol group site to which an ethanol molecule can be strongly hydrogen-bonded, and the other is the siloxane (Si−O−Si) group site to which an ethanol molecule can be weakly bonded. The presence of water in vapor significantly reduced the surface coverage of ethanol on silica due to competitive adsorption between ethanol and water.

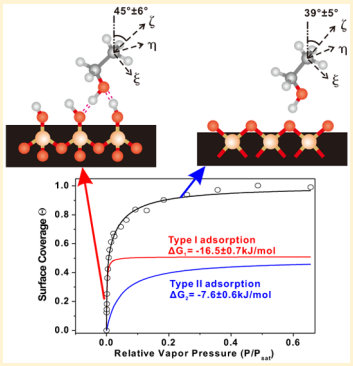

INTRODUCTION

Being a simple amphiphilic molecule, alcohol on a solid interface is of interest as it plays a key role in adhesion,[1,2] catalysis,[3−5] wetting,[6−8] and tribology.[9−12] Alcohol decorating the glass surface and modifying the wetting behavior of the surface is believed to be responsible for the mysterious tears of wine on glass.[13,14] Adsorption of alcohol on silicon oxide significantly reduces friction and wear of the oxide surface,[9−12] whereas water gives rise to large friction considered deleterious in semiconductor nanotechnology. Understanding the adsorption structure and process of alcohol molecules on fused silica at the molecular level is clearly desired.

Adsorption of amphiphilic molecules, such as alcohol, on fused silica depends on the available adsorption sites on the surface of silica. The α-quartz(0001) surface is known to be composed of siloxane (Si−O−Si) and silanol (Si−OH) groups,[15] the ratio of which depends on the surface preparation. These surface groups presumably also comprise a surface of fused silica, although the crystalline Si−O−Si surface phonon mode was not observable in the surface vibrational spectra of silica.[16−18] There are suggestions that some surface hydroxyls may also have their H bonded to a neighboring O,[16,18,19] but they cannot be identified in the surface spectra. Both alcohol and water molecules can adsorb on surface sites of silica by hydrogen (H)-bonding. We are first interested in the alcohol adsorption from the gas phase in the absence of water, which can serve as a reference for the study of whether adsorption of alcohol and water is competitive or cooperative. The latter is needed for understanding how the surface friction of silica decorated by alcohol would change when prepared in a dry or wet environment.[9−12]

A number of techniques have been used to study adsorbates on solid surfaces. AFM and SEM are excellent tools for imaging and measuring the friction coefficient of alcohol vapor/fused silica interfaces,[9,10,12,20] but they are unable to provide information on the molecular structure. Modern IR spectroscopy can yield vibrational spectra of alcohol molecules on a fused silica surface.[21,22] Adsorbed layer thickness and average molecular conformation could be deduced from the spectra. The technique is, however, not surface specific and suffers from background contribution from the bulk. Its sensitivity is limited to a monolayer (ML) or more.[23,24]

Sum-frequency vibrational spectroscopy (SFVS) as a surface probe has high sensitivity and surface specificity to detect vibrational spectra of a submonolayer of adsorbed molecules on

Special Issue: Mario Molina Festschrift

Received: October 24, 2014
Revised: December 17, 2014
Published: January 12, 2015

DOI: 10.1021/jp510706u
J. Phys. Chem. A 2015, 119, 4573−4580

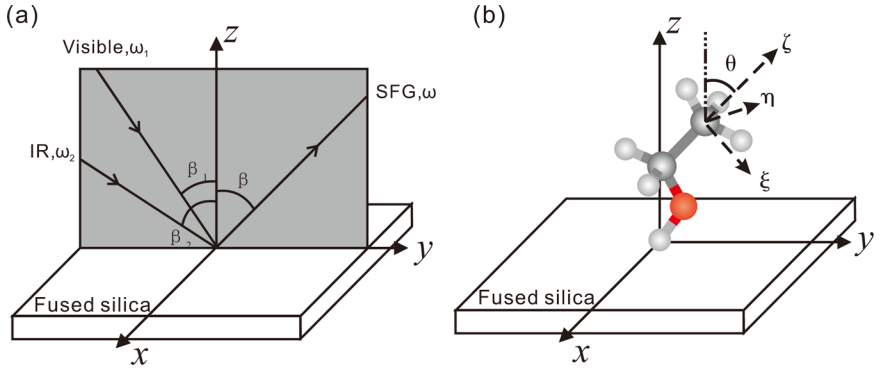

Figure 1. (a) Beam geometry in the SF measurement. (b) Description of the orientation of an ethanol molecule in the lab and molecular coordinates.

a surface or buried interface.[25−31] The polarization-dependent spectra also allow determination of polar orientation of selected chemical groups of adsorbates on a surface. Adsorption energy of adsorbates can be obtained from the adsorption isotherm deduced from the measured spectra versus the vapor pressure of the adsorbates. Liu et al. used SFVS to study alcohol adsorption at both gas/silica and liquid/silica interfaces.[32] However, in their gas experiment, humidity was not controlled and possible competitive adsorption of water was not discussed.

In this paper, we report a SFVS study on ethanol adsorption on fused silica at the vapor/solid interface by carefully controlling the vapor pressures of ethanol and water in nitrogen gas at room temperature (22 °C). The ethanol partial pressure was varied from $0.0001P_{sat}$ to $0.89P_{sat}$ in dry nitrogen carrier gas, where P_{sat} denotes the saturation pressure. Adsorbed ethanol molecules appeared to form a nearly full monolayer on silica when the ethanol vapor pressure was above $0.35P_{sat}$. The orientational angle of the methyl group of ethanol changed from 45° ± 6° with respect to the surface normal at low coverage to 39° ± 5° at high coverage. Two distinct adsorption processes were identified with adsorption energies of −16.5 ± 0.7 kJ/mol (type I) and −7.6 ± 0.6 kJ/mol (type II), and saturated surface populations of 51% ± 5% and 49% ± 5% of a monolayer, respectively. Phase sensitive-SFVS reveals that the stronger type I adsorption is associated with the silanol sites on the silica surface, and the weaker type-II adsorption is associated with Si−O−Si. With the presence of water, ethanol and water molecules competitively adsorb on silica. Qualitatively, the adsorption strength of water molecules is comparable to that of ethanol molecules on fused silica with the latter being somewhat larger.

THEORETICAL BASIS

The basic theory of SFVS for interface studies has been described in detail elsewhere.[25,33−35] Briefly, the reflected SF ($\omega = \omega_1 + \omega_2$) output from an interface is given by

$$S(\omega=\omega_1+\omega_2) \propto |[\vec{L}(\omega)\cdot\hat{e}]\cdot\vec{\chi}_s^{(2)}:[\hat{e}_1\cdot\vec{L}(\omega_1)][\hat{e}_2\cdot\vec{L}(\omega_2)]|^2 I_1 I_2 = |\chi_{eff}^{(2)}|^2 I_1 I_2 \quad (1)$$

where I_1 and I_2 are input beam intensities at ω_1 and ω_2 and $\vec{L}(\omega_i)$ and $\hat{e}_i$ denote the Fresnel transmission coefficient tensor and unit polarization vector at ω_i, respectively. The surface nonlinear susceptibility $\vec{\chi}_S^{(2)}$, assuming discrete resonances, can be expressed as

$$\chi_{S,ijk}^{(2)} = \chi_{NR,ijk}^{(2)} + \sum_q \frac{A_{q,ijk}}{\omega_2 - \omega_q + i\Gamma_q} \quad (2)$$

and

$$\mathrm{Im}\,\chi_{S,ijk}^{(2)} = -\sum_q \frac{A_{q,ijk}\Gamma_q}{(\omega_2 - \omega_q)^2 + \Gamma_q^2} \quad (3)$$

Here, $\chi_{NR,ijk}^{(2)}$ denotes the nonresonant contribution and $A_{q,ijk}$ is the amplitude of the qth vibrational mode at frequency ω_q with damping constant Γ_q. The sign of $\mathrm{Im}\,\chi_{S,ijk}^{(2)}$ is related to the absolute orientation of surface species. Different input/output polarization combinations allow deduction of molecular orientation.[23,36,37]

Figure 1 shows the beam geometry and definition of ethanol molecular orientation in the lab (x, y, z) and molecular (ξ, η, ζ) coordination systems, respectively. For ethanol on fused silica, the interface is azimuthally isotropic ($C_{\infty v}$). The effective nonlinear susceptibility $\chi_{eff,\hat{e}\hat{e}_1\hat{e}_2}^{(2)}$ for the four polarization combinations, ssp, sps, pss, and ppp, can be expressed in terms of the independent nonvanishing surface susceptibility elements $\chi_{S,ijk}^{(2)}$:

$$\chi_{eff,ssp}^{(2)} = L_{yy}(\omega)\, L_{yy}(\omega_1)\, L_{zz}(\omega_2) \sin\beta_2 \chi_{S,yyz}^{(2)}$$

$$\chi_{eff,sps}^{(2)} = L_{yy}(\omega)\, L_{zz}(\omega_1)\, L_{yy}(\omega_2) \sin\beta_1 \chi_{S,yzy}^{(2)}$$

$$\chi_{eff,pss}^{(2)} = L_{zz}(\omega)\, L_{yy}(\omega_1)\, L_{yy}(\omega_2) \sin\beta \chi_{S,zyy}^{(2)}$$

$$\begin{aligned}\chi_{eff,ppp}^{(2)} = {} & -L_{xx}(\omega)\, L_{xx}(\omega_1)\, L_{zz}(\omega_2) \cos\beta \cos\beta_1 \sin\beta_2 \chi_{S,xxz}^{(2)} \\ & - L_{xx}(\omega)\, L_{zz}(\omega_1)\, L_{xx}(\omega_2) \cos\beta \sin\beta_1 \cos\beta_2 \chi_{S,xzx}^{(2)} \\ & + L_{zz}(\omega)\, L_{xx}(\omega_1)\, L_{xx}(\omega_2) \sin\beta \cos\beta_1 \cos\beta_2 \chi_{S,zxx}^{(2)} \\ & + L_{zz}(\omega)\, L_{zz}(\omega_1)\, L_{zz}(\omega_2) \sin\beta \sin\beta_1 \sin\beta_2 \chi_{S,zzz}^{(2)}\end{aligned} \quad (4)$$

The surface susceptibility $\vec{\chi}_S^{(2)}$ in the lab coordinates is related to the nonlinear hyperpolarizability $\vec{\alpha}^{(2)}$ in the molecular coordinates by

$$\chi_{S,ijk}^{(2)} = N_s \sum_{\xi\eta\zeta} \langle(\hat{i}\cdot\hat{\xi})(\hat{j}\cdot\hat{\eta})(\hat{k}\cdot\hat{\zeta})\rangle \alpha_{\xi\eta\zeta}^{(2)} \quad (5)$$

where N_s is the surface density of adsorbates and the angular brackets denote an average over molecular orientations. For the methyl group with C_{3v} symmetry, the nonvanishing elements of $\vec{\alpha}^{(2)}$ are[36−38]

DOI: 10.1021/jp510706u
J. Phys. Chem. A 2015, 119, 4573−4580

$$\alpha^{(2)}_{\zeta\zeta\zeta}$$
$$\alpha^{(2)}_{\xi\xi\zeta} = \alpha^{(2)}_{\eta\eta\zeta}$$
$$\alpha^{(2)}_{\xi\zeta\xi} = \alpha^{(2)}_{\eta\zeta\eta} \approx \alpha^{(2)}_{\zeta\xi\xi} = \alpha^{(2)}_{\zeta\eta\eta}$$
$$\alpha^{(2)}_{\xi\xi\xi} = -\alpha^{(2)}_{\eta\eta\xi} = -\alpha^{(2)}_{\xi\eta\eta} = -\alpha^{(2)}_{\eta\xi\eta} \quad (6)$$

We then have[23,36−38]

$$\chi^{(2),ss}_{S,xxz} = \chi^{(2),ss}_{S,yyz} = \frac{1}{2}N_s\alpha^{(2)}_{\zeta\zeta\zeta}[\langle\cos\theta\rangle(1+r) - \langle\cos^3\theta\rangle(1-r)]$$
$$\chi^{(2),ss}_{S,xzx} = \chi^{(2),ss}_{S,yzy} = \chi^{(2),ss}_{S,zxx} = \chi^{(2),ss}_{S,zyy} = \frac{1}{2}N_s\alpha^{(2)}_{\zeta\zeta\zeta}(\langle\cos\theta\rangle - \langle\cos^3\theta\rangle)(1-r)$$
$$\chi^{(2),ss}_{S,zzz} = N_s\alpha^{(2)}_{\zeta\zeta\zeta}[r\langle\cos\theta\rangle + \langle\cos^3\theta\rangle(1-r)] \quad (7)$$

for the symmetric stretch, and

$$\chi^{(2),as}_{S,xxz} = \chi^{(2),as}_{S,yyz} = -N_s\alpha^{(2)}_{\zeta\xi\xi}(\langle\cos\theta\rangle - \langle\cos^3\theta\rangle)$$
$$\chi^{(2),as}_{S,xzx} = \chi^{(2),as}_{S,yzy} = \chi^{(2),as}_{S,zxx} = \chi^{(2),as}_{S,zyy} = N_s\alpha^{(2)}_{\zeta\xi\xi}\langle\cos^3\theta\rangle$$
$$\chi^{(2),as}_{S,zzz} = 2N_s\alpha^{(2)}_{\zeta\xi\xi}(\langle\cos\theta\rangle - \langle\cos^3\theta\rangle) \quad (8)$$

for the asymmetric stretch. Here, $r = \alpha^{(2)}_{\xi\xi\zeta}/\alpha^{(2)}_{\zeta\zeta\zeta}$ is the depolarization ratio and θ is the polar angle of the symmetry axis ζ with respect to the z-axis. From the polarization-dependent spectra, $\chi^{(2)}_{S,zzz}/\chi^{(2)}_{S,yyz}$ and $\chi^{(2)}_{S,xzx}/\chi^{(2)}_{S,yyz}$, or the corresponding amplitude ratios of $A_{q,ijk}$ for different modes, can be deduced, and then from eq 7 or 8, the orientational angle θ and the depolarization ratio r can be determined.[23,37] With the orientation angle, the relative N_s can then be deduced from the ratio of $\chi^{(2)}_{S,ijk}$ at different surface coverages.

Following the simple Langmuir adsorption model, the expression of the adsorption isotherm is[31,39]

$$\Theta = x/(x + e^{-\Delta G/RT}) \quad (9)$$

if there is only one kind of adsorption site, and[19,40]

$$\Theta = \frac{Ax}{x + e^{-\Delta G_1/RT}} + \frac{(1-A)x}{x + e^{-\Delta G_2/RT}} \quad (10)$$

if there are two kinds of adsorption sites, where $\Theta \equiv N_s/N_{s,sat}$ with $N_{s,sat}$ being the saturated surface density of adsorbates, $x = P/P_{sat}$, and A and $(1-A)$ are the relative fractions of the type I and type II surface sites, respectively.[19,31,39,40] Here, the air/liquid ethanol interface is chosen as the reference system. The Gibbs adsorption free energy ΔG_i can be deduced from the fitting of the isotherm curve.

EXPERIMENTAL SECTION

A 5 mm thick fused silica was cleaned by soaking in a mixture of concentrated sulfuric acid (98%) and Nochromix (DODAX Laboratories Inc.) for more than 3 h, then rinsed thoroughly with deionized water (with a resistivity of 18.2 MΩ·cm), and finally blown dry with filtered nitrogen gas and placed into a sealed chamber purged and filled with N_2 for optical measurement.

Ethanol of the HPLC grade was purchased from Aladdin (≥99.8%). The experimental setup is described in Figure 2.

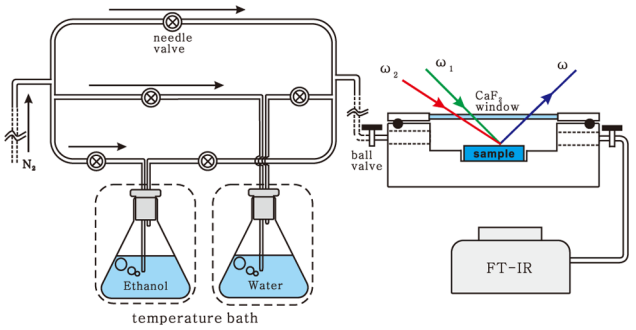

Figure 2. Sketch of the experimental setup.

Composition of N_2 and ethanol in the gas mixture was controlled by controlling the flow rates of pure nitrogen gas (ultrapure grade, 99.9999%) and nitrogen gas saturated with ethanol at different bath temperatures. The mixture was sent through a long tube to reach the sample chamber to ensure homogeneity. Composition of the gas mixture in the chamber was monitored by an FTIR spectrometer. A separate gas line with N_2 flowing through water in a thermal bath at a controlled rate was used to control humidity of the gas mixture in the chamber. The humidity was measured by a hygrometer (Testo 608-H2) and the FTIR spectrometer.

The SFVS setup employed was a picosecond system similar to that described earlier.[41−44] Noncollinear beam geometry with IR and visible inputs at incident angles of 57° and 45°, respectively, was used for SFVS intensity measurements and collinear beam geometry for phase-sensitive SFVS measurements. All the spectra were normalized against the SF signal from a z-cut quartz with the same experimental parameters.

RESULTS AND DISCUSSION

Figure 3a shows a set of ssp (s-, s-, and p-polarized SF, visible, and IR beams, respectively) $|\chi^{(2)}_{S,ssp}|^2$ spectra in the CH stretch region for ethanol adsorbed on fused silica at different ethanol partial pressures and 0% humidity. The strong CH stretching spectra suggest that the adsorbed ethanol molecules are well polar-oriented. Spectral features could be observed even when the ethanol partial pressure was down to 0.6 Pa ($0.0001P_{sat}$). The peaks at 2874 and 2930 cm^{-1} can be assigned to the symmetric stretching mode (r^+) and the Fermi resonance (r^+-FR) of the methyl ($-CH_3$) group, respectively.[36,45] Their intensities increase with the ethanol partial pressure (P) and approach a maximum when $P \sim 0.35P_{sat}$, suggesting near saturation of adsorption at a full monolayer coverage. This result is consistent with those of friction experiments under alcohol atmosphere, which also showed that the friction coefficient stopped changing for $P \geq 0.35P_{sat}$.[9,11] The spectrum then remains unchanged up to $0.89P_{sat}$, indicating multilayer adsorption of ethanol on fused silica has not yet occurred. The spectra in Figure 3a are clearly different from that of the liquid ethanol/fused silica interface reported earlier.[31] After all, ethanol adsorbed at vapor/silica and liquid/silica interfaces should adopt different structures.

For quantitative analysis, decomposition of the SF spectra into discrete modes is needed. Displayed in Figure 3b is the $\mathrm{Im}\,\chi^{(2)}_{S,ssp}$ spectrum of ethanol on fused silica under an ethanol partial pressure of $0.128P_{sat}$ obtained by phase-sensitive SFVS. Global fitting of both $|\chi^{(2)}_{S,ssp}|^2$ and $\mathrm{Im}\,\chi^{(2)}_{S,ssp}$ spectra allows unique decomposition and characterization of the different modes including their signs. Five modes appear through the fitting, as

DOI: 10.1021/jp510706u
J. Phys. Chem. A 2015, 119, 4573−4580

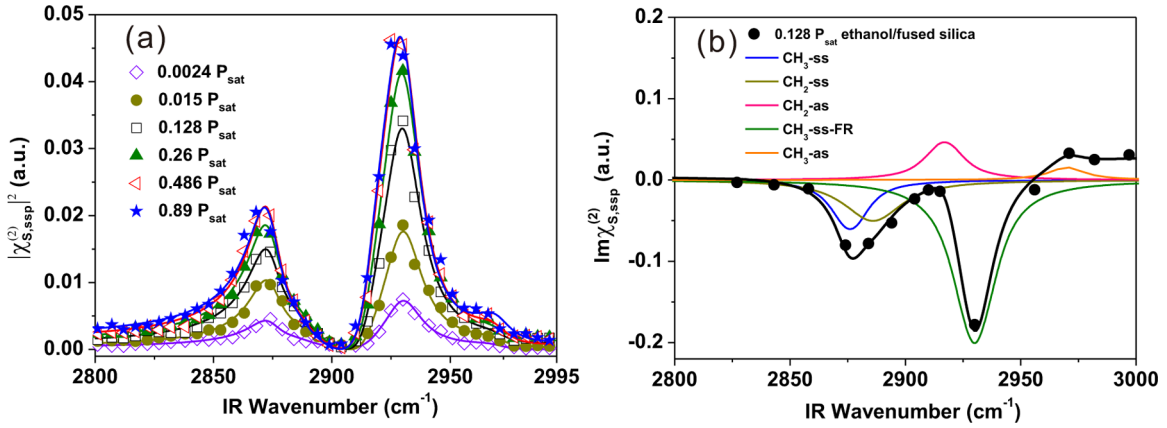

Figure 3. (a) ssp $|\chi^{(2)}_{S,ssp}|^2$ spectra of the vapor/fused silica interface as a function of ethanol vapor pressure from $0.0024P_{sat}$ to $0.89P_{sat}$. The saturation vapor pressure of ethanol at 22 °C is 6615 Pa. The solid curves are fitting results using eqs 2 and 3. (b) Im $\chi^{(2)}_{S,ssp}$ spectrum of the vapor/fused silica interface at ethanol vapor pressure of $0.128P_{sat}$. The thick solid curve is the global fitting result of both Im $\chi^{(2)}_{S,ssp}$ and $|\chi^{(2)}_{S,ssp}|^2$ spectra. The thin lines are the five resonant modes deduced from fitting.

shown in Figure 3b. Their characteristic parameters are listed in Table 1. Following the assignment of refs 36 and 45, we attribute the strong negative modes at 2874, 2886, and 2930 cm^{-1} to the r^+ mode of CH_3, symmetric stretch (d^+) of CH_2, and r^+-FR of CH_3, respectively, and the positive bands at 2970 and 2917 cm^{-1} to the asymmetric stretch (r^-) of CH_3 and the asymmetric stretch (d^-) of CH_2. The negative sign of the r^+ mode corresponds to CH_3 pointing toward air, opposite to the case of OH.[46] We can fit all $|\chi^{(2)}_{S,ssp}|^2$ spectra obtained under different ethanol pressures with different polarization combinations (ssp, sps, ppp) using these five discrete modes with their signs, resonant frequencies, and damping constants all fixed, but their mode strength adjustable.

Table 1. Characteristic Constants of the Five Discrete Modes Obtained by Fitting of the SFVS Spectrum of Adsorbed Ethanol on Fused Silica at $0.128P_{sat}$ Ethanol Partial Vapor Pressure

mode	ω_q (cm^{-1})	Γ_q (cm^{-1})	$A_{q,ssp}$
r^+	2874	8.2	−0.55 ± 0.03
d^+	2886	14.3	−0.75 ± 0.06
d^-	2917	8.8	0.45 ± 0.02
r^+-FR	2930	9.9	−2.13 ± 0.02
r^-	2970	9.4	0.15 ± 0.04

As described earlier, we can deduce the average orientation of adsorbed ethanol molecules from the SF vibrational spectra of different polarization combinations. To see if the orientation changes with surface coverage, the ssp, sps, and ppp SF spectra of adsorbed ethanol on silica at ethanol partial pressures of $0.0069P_{sat}$ (corresponding to much less than a full adsorbed monolayer) and $0.66P_{sat}$ (corresponding to a nearly full adsorbed monolayer) were measured. They are plotted in Figure 4a,b. The significantly weaker r^+ and r^+-FR resonance modes in the sps spectra indicate that the symmetry axis of the methyl group is more inclined toward the surface normal. Quantitatively, fitting of the spectra yields values of A_{ssp}, A_{sps}, and A_{ppp} for the different modes. We focused on the r^- mode and used eq 8 to deduce the orientation of CH_3 because of its better signal-to-noise ratio in the spectra of different polarizations. (Close overlapping of the r^+ and d^+ modes also causes larger errors in deduction of their amplitudes.) By assuming $\delta(\theta - \theta_0)$ for the orientation distribution, we found, from the values of $A^{(2)}_{ppp}/A^{(2)}_{ssp}$ and $A^{(2)}_{sps}/A^{(2)}_{ssp}$, that $\theta_0 = 45° \pm 6°$ and $39° \pm 5°$ at $0.0069P_{sat}$ and $0.66P_{sat}$ using eq 8, respectively, and also $r = 1.8$ using eq 7, which roughly agrees with values reported in the literature.[23,47−49] (An analysis based on the assumption of a Gaussian orientation distribution is described in the Supporting

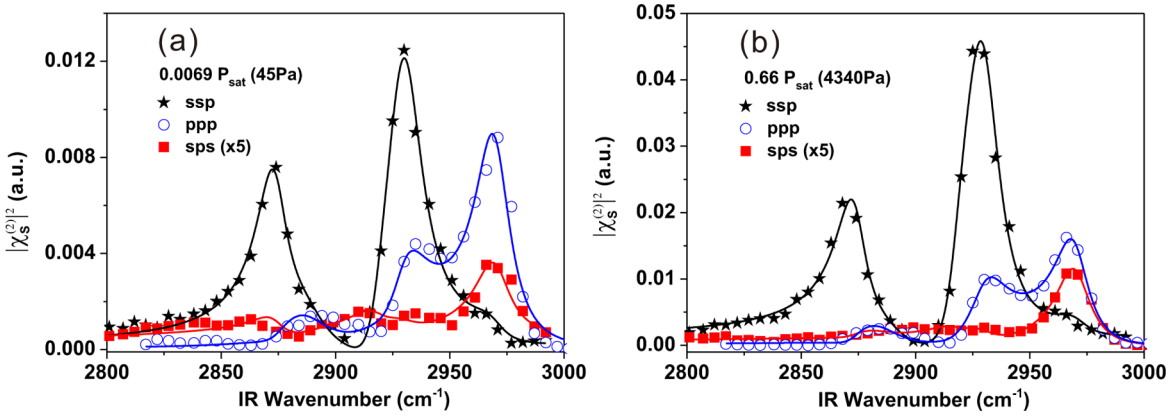

Figure 4. ssp, ppp, and sps $|\chi^{(2)}_S|^2$ spectra for the vapor/fused silica interface in the CH stretch range at an ethanol vapor pressure of (a) $0.0069P_{sat}$ and (b) $0.66P_{sat}$, respectively. The sps spectra are enlarged 5 times for better comparison.

DOI: 10.1021/jp510706u
J. Phys. Chem. A 2015, 119, 4573−4580

Information.) The result on the orientation is consistent with that of Liu et al.,[32] but inconsistent with the ATR-IR result by Barnette et al. at low vapor pressure.[21] The latter appeared to have poor accuracy in the submonolayer region. Our analysis of the r^+ mode also provided consistent result for the orientation of CH_3, but with larger errors.

The surface coverage, $\Theta = N_S/N_{S,sat}$, of alcohol adsorbates on silica versus the ethanol relative partial pressure, P/P_{sat}, can also be deduced from the spectra with reference to the full monolayer at $P > 0.35P_{sat}$. This yields the adsorption isotherm shown in Figure 5, which can be best fit by eq 10 for the two-site Langmuir adsorption model with Gibbs adsorption energies $\Delta G_1 = -16.5 \pm 0.7$ kJ/mol and $\Delta G_2 = -7.6 \pm 0.6$ kJ/mol, and fractions of the two sites, $A = 51 \pm 5\%$ and $(1 - A) = 49 \pm 5\%$, respectively. Note that the relative abundance of the two sites may depend on the surface preparation method. The stronger adsorption (type I) of ethanol is likely to happen at the silanol sites and the weaker one (type II) at the Si−O−Si sites. The result does not allow us to identify the presence of two silanol adsorption sites on silica with different adsorption energies.

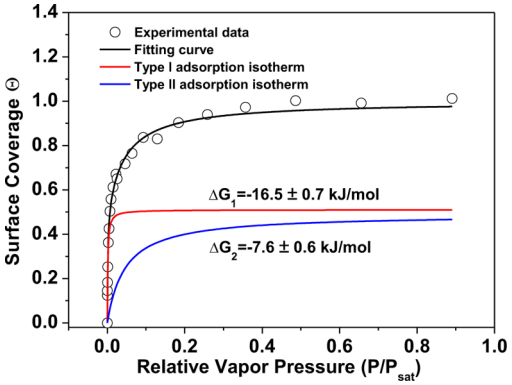

Figure 5. Adsorption isotherm of gaseous ethanol adsorbed on fused silica at 0% RH. The *x*-axis is the relative vapor pressure, P/P_{sat}. The red and the blue curves are the type I and the type II components of the adsorption isotherm, respectively.

We have recorded the OH stretch spectra together with the CH stretch spectra of adsorbed ethanol by SFVS. Figure 6a presents the OH intensity spectra of the vapor/fused silica interface at zero and 0.85 ML ($P = 0.128P_{sat}$) of ethanol coverage with 0% humidity, respectively. For freshly prepared fused silica surface in dry nitrogen, the sharp peak positioned at 3750 cm^{-1} is readily identified as the dangling silanol group (Si−OH) on the surface. As ethanol vapor pressure gradually increases, the silanol peak becomes weaker and eventually disappears (Figure 7a), while a broad band from 3000 to 3600 cm^{-1} in the bonded OH stretch region grows. The disappearance of the dangling OH peak is an indication of ethanol H-bonded to the silanol sites. This can be seen as the type-I adsorption process mentioned above, as will be further confirmed later. The Im $\chi^{(2)}_{S,ssp}$ spectrum for 0.85 ML of ethanol adsorption is shown in Figure 6b. It is seen that the broad band is composed of two sub-bands, one positive from 3000 to 3400 cm^{-1} and the other negative from 3400 to 3600 cm^{-1}, where the positive band in Im $\chi^{(2)}_{S,ssp}$ refers to O → H pointing toward air. The negative band is hardly detectable below an ethanol surface coverage of ~0.5 ML (at $P = 0.0056P_{sat}$, Figure 6b), at which the type-II adsorption process is still insignificant. The negative band therefore must originate from the downward pointing OH of ethanol molecules adsorbed on silica by the type-II adsorption process. The adsorption is likely to be at the siloxane sites and is weak, judging from the higher OH stretching frequencies, consistent with the weak adsorption energy $\Delta G_2 = -7.6 \pm 0.6$ kJ/mol found earlier. The positive band of 3000−3400 cm^{-1} comes mainly from the up-pointing OH of silanol. Adsorption of ethanol by hydrogen bonding on silanol eliminates the dangling Si−OH and changes its sharp OH peak into an inhomogeneously broadened band at lower frequency. The down-pointing OH of the adsorbed ethanol should contribute negatively to this broad band, but its contribution may be less than that of the silanol because of its larger tilt toward the surface.

To better understand how ethanol adsorbs on the silanol sites, we deduced the surface coverage of the dangling OH of silanol as a function of the ethanol vapor pressure from the observed dangling Si−OH peak at 3750 cm^{-1} in the spectra. The amplitude of the dangling Si−OH peak versus P/P_{sat} is plotted in Figure 7a. It is seen that as the ethanol partial pressure increases, the amplitude of the dangling silanol group drastically decreases and eventually disappears when the ethanol coverage reaches ~0.5 ML. By normalizing the amplitude of the dangling Si−OH mode at different ethanol pressures against that without ethanol, we can obtain the surface coverage of the empty silanol sites, Θ_{sil}, or the occupied

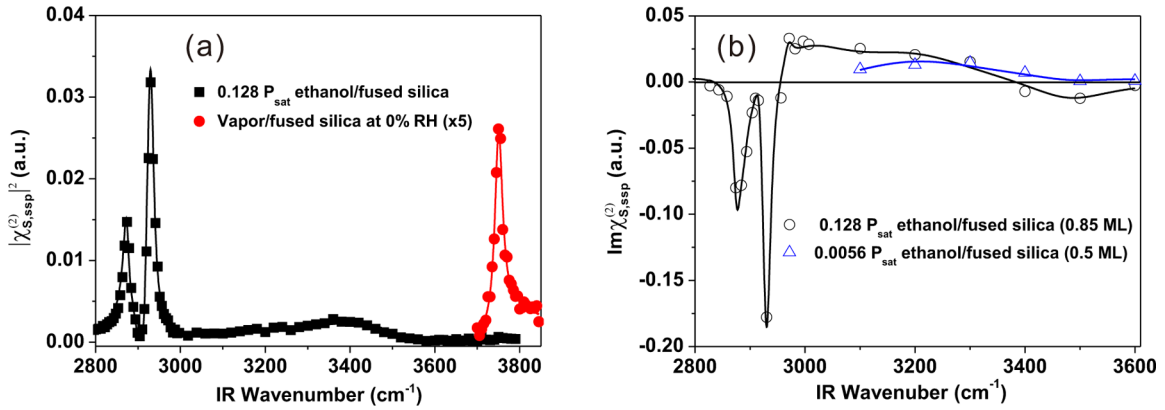

Figure 6. (a) ssp $|\chi^{(2)}_{S,ssp}|^2$ spectra of adsorbed ethanol on fused silica in the CH and OH stretch range at ethanol vapor pressures of 0 and $0.128P_{sat}$, respectively. The spectrum of the dangling silanol group on the surface is enlarged 5 times. (b) ssp Im $\chi^{(2)}_{S,ssp}$ spectra of adsorbed ethanol on fused silica at ethanol vapor pressures of $0.128P_{sat}$ (0.85 ML) and $0.0056P_{sat}$ (0.5 ML), respectively.

DOI: 10.1021/jp510706u
J. Phys. Chem. A 2015, 119, 4573−4580

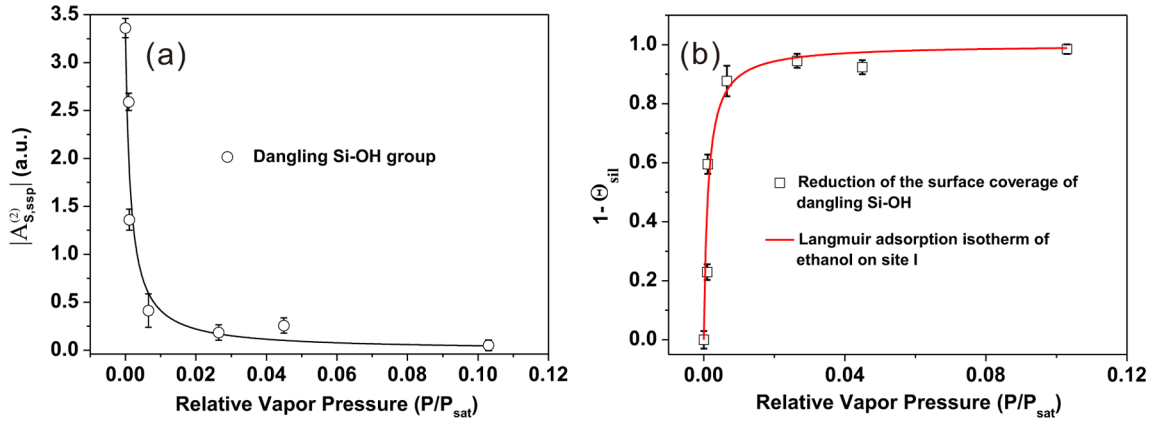

Figure 7. (a) Amplitude of the dangling Si−OH mode versus normalized ethanol vapor pressure. (b) Reduction of the dangling silanol sites, $1 - \Theta_{sil}$, versus P/P_{sat}, where Θ_{sil} denotes the surface coverage of the empty silanol sites. The solid curve is the calculated Langmuir adsorption isotherm using $\Delta G_1 = -16.5$ kJ/mol obtained from the fitting of the type I adsorption in Figure 5.

silanol sites, $1 - \Theta_{sil}$, as a function of P/P_{sat}. The result is plotted in Figure 7b and is seen to fit well with the same Langmuir adsorption isotherm presented in Figure 5 for type-I adsorption with $\Delta G_1 = -16.5$ kJ/mol. Thus, we can conclude that ethanol adsorption on the silanol sites is indeed responsible for the type-I adsorption process. In this spectral investigation of the OH stretch range, again we are unable to identify contribution from other silanol sites to ethanol adsorption. This suggests that either the surface density of the other silanol sites is small, or the adsorption probability of ethanol on such sites is small, or ethanol adsorption on such sites is nearly identical to adsorption on the dangling silanol sites.

We now discuss briefly the water effect on ethanol adsorption on fused silica. First, we found that the residual water adsorption on our dry silica surface is not significant, as described and explained in the Supporting Information. Figure 8 then shows the SF intensity spectra of the CH stretches with

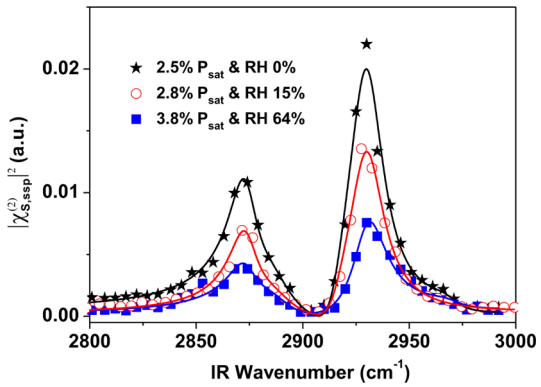

Figure 8. ssp $|\chi^{(2)}_{S,ssp}|^2$ spectra of vapor/fused silica interface at different partial pressures of ethanol and water.

and without the presence of water in the vapor. The surface coverage of ethanol is ~0.65 ML under an ethanol vapor pressure of $0.025P_{sat}$ (165 Pa) and 0% relative humidity (RH) but is reduced by ~25% (deduced from the mode amplitude A_q) at 15% RH (corresponds to 400 Pa of water partial pressure). This is an indication of competitive adsorption of water and ethanol on fused silica. From the equation for competitive Langmuir adsorption of two species on a surface,[39,50] we can conclude that the adsorption energies of ethanol and water are comparable, but that of ethanol is higher. When the RH is increased up to 64%, which is close to that of the outdoor atmosphere in many places, the CH signal becomes a few times smaller than that in a dry environment. Thus, if the fused silica surface is treated in alcohol vapor under ambient condition, the higher the RH, the less alcohol will appear on the surface which in turn will lead to high friction and serious wearing of the surface. A detailed study of competitive adsorption of ethanol and water on silica is currently in progress.

CONCLUSION

We have used SFVS in the CH and OH stretch region to probe adsorption of ethanol on fused silica and its dependence on ethanol vapor pressure in N_2 carrier gas. Adsorption associated with two distinct adsorption sites on silica was identified. Under low ethanol vapor pressure, adsorption was dominated by hydrogen bonding between the hydroxyl group of ethanol and the silanol group on silica with an adsorption energy of −16.5 ± 0.7 kJ/mol. Hydrogen bonding in the adsorption is manifested by the appearance of the bonded OH stretches between 3000 and 3400 cm^{-1}. Under high ethanol vapor pressure, another adsorbed ethanol species weakly bonded to the siloxane group on silica appeared with an adsorption energy of −7.6 ± 0.6 kJ/mol and was accompanied by the emergence of a weak bonded OH band between 3400 and 3600 cm^{-1}. The two types of adsorption sites occupied, respectively, 51 ± 5% and 49 ± 5% of the silica surface of our sample. The average orientation of the methyl group of adsorbed ethanol changed from 45° ± 6° to 39° ± 5° as the ethanol vapor pressure increased. We also found that water and ethanol molecules adsorbed competitively on silica with ethanol having slightly higher adsorption energy. This study provides molecular-level structural information on ethanol adsorption on an oxide surface, and may have relevance to technology including tribology.

ASSOCIATED CONTENT

Supporting Information

Calculation of orientation distribution by the Gaussian distribution function; OH sum-frequency vibrational spectra of the fused silica surface at different humidities and baked at 200 °C. This material is available free of charge via the Internet at http://pubs.acs.org.

DOI: 10.1021/jp510706u
J. Phys. Chem. A 2015, 119, 4573−4580

AUTHOR INFORMATION

Corresponding Authors

*C. Tian. E-mail: cstian@fudan.edu.cn.

*R. Shen. E-mail: yrshen@calmail.berkeley.edu.

Notes

The authors declare no competing financial interest.

ACKNOWLEDGMENTS

C.S.T. acknowledges support by the NSFC (No. 11374064, No.11290161, and No. 11104034), NCET, and Shanghai Pujiang Program (No. 12PJ1400900). Y.R.S. acknowledges support from the Director, Office of Science, Office of Basic Energy Sciences, Materials Sciences and Engineering Division, of the U.S. Department of Energy, under Contract No. DE-AC03-76SF00098.

REFERENCES

(1) Pelmenschikov, A. G.; Morosi, G.; Gamba, A.; Zecchina, A.; Bordiga, S.; Paukshtis, E. A. Mechanisms of Methanol Adsorption on Silicalite and Silica - IR-Spectra and Ab-Initio Calculations. *J. Phys. Chem.* **1993**, *97*, 11979−11986.

(2) Natal-Santiago, M. A.; Dumesic, J. A. Microcalorimetric, FTIR, and DFT Studies of the Adsorption of Methanol, Ethanol, And 2,2,2-Trifluoroethanol on Silica. *J. Catal.* **1998**, *175*, 252−268.

(3) Kawai, T.; Sakata, T. Photocatalytic Hydrogen-Production from Liquid Methanol and Water. *J. Chem. Soc. Chem. Comm.* **1980**, 694−695.

(4) Pang, C. L.; Lindsay, R.; Thornton, G. Chemical Reactions on Rutile TiO_2(110). *Chem. Soc. Rev.* **2008**, *37*, 2328−2353.

(5) Seddon, D. Reformulated Gasoline, Opportunities for New Catalyst Technology. *Catal. Today* **1992**, *15*, 1−21.

(6) Hare, E. F.; Zisman, W. A. Autophobic Liquids and the Properties of Their Adsorbed Films. *J. Phys. Chem.* **1955**, *59*, 335−340.

(7) Ulman, A.; Evans, S. D.; Shnidman, Y.; Sharma, R.; Eilers, J. E.; Chang, J. C. Concentration-Driven Surface Transition in the Wetting of Mixed Alkanethiol Monolayers on Gold. *J. Am. Chem. Soc.* **1991**, *113*, 1499−1506.

(8) Bain, C. D.; Whitesides, G. M. A Study by Contact Angle of the Acid-Base Behavior of Monolayers Containing. Omega.-Mercaptocarboxylic Acids Adsorbed on Gold: An Example of Reactive Spreading. *Langmuir* **1989**, *5*, 1370−1378.

(9) Strawhecker, K.; Asay, D. B.; McKinney, J.; Kim, S. H. Reduction of Adhesion and Friction of Silicon Oxide Surface in the Presence of n-Propanol Vapor in the Gas Phase. *Tribol. Lett.* **2005**, *19*, 17−21.

(10) Asay, D. B.; Dugger, M. T.; Ohlhausen, J. A.; Kim, S. H. Macro- to Nanoscale Wear Prevention via Molecular Adsorption. *Langmuir* **2008**, *24*, 155−159.

(11) Asay, D. B.; Dugger, M. T.; Kim, S. H. In-Situ Vapor-Phase Lubrication of MEMS. *Tribol. Lett.* **2008**, *29*, 67−74.

(12) Barnette, A. L.; Asay, D. B.; Kim, D.; Guyer, B. D.; Lim, H.; Janik, M. J.; Kim, S. H. Experimental and Density Functional Theory Study of the Tribochemical Wear Behavior of SiO_2 in Humid and Alcohol Vapor Environments. *Langmuir* **2009**, *25*, 13052−13061.

(13) Fournier, J.; Cazabat, A. Tears of Wine. *Europhys. Lett.* **1992**, *20*, 517.

(14) Vuilleumier, R.; Ego, V.; Neltner, L.; Cazabat, A. Tears of Wine: The Stationary State. *Langmuir* **1995**, *11*, 4117−4121.

(15) Liu, W. T.; Shen, Y. R. Surface Vibrational Modes of Alpha-Quartz(0001) Probed by Sum-Frequency Spectroscopy. *Phys. Rev. Lett.* **2008**, *101*, 016101.

(16) Iler, R. K. *The Chemistry of Silica*; Wiley-Interscience: New York, 1978; pp 623, 630.

(17) Isaienko, O.; Borguet, E. Hydrophobicity of Hydroxylated Amorphous Fused Silica Surfaces. *Langmuir* **2013**, *29*, 7885−7895.

(18) Ong, S. W.; Zhao, X. L.; Eisenthal, K. B. Polarization of Water-Molecules at a Charged Interface - 2nd Harmonic Studies of the Silica Water Interface. *Chem. Phys. Lett.* **1992**, *191*, 327−335.

(19) Dong, Y.; Pappu, S. V.; Xu, Z. Detection of Local Density Distribution of Isolated Silanol Groups on Planar Silica Surfaces Using Nonlinear Optical Molecular Probes. *Anal. Chem.* **1998**, *70*, 4730−4735.

(20) Kanda, Y.; Nakamura, T.; Higashitani, K. AFM Studies of Interaction Forces between Surfaces in Alcohol-Water Solutions. *Colloids Surf., A: Physicochem. Eng. Aspects* **1998**, *139*, 55−62.

(21) Barnette, A. L.; Asay, D. B.; Janik, M. J.; Kim, S. H. Adsorption Isotherm and Orientation of Alcohols on Hydrophilic SiO_2 under Ambient Conditions. *J. Phys. Chem. C* **2009**, *113*, 10632−10641.

(22) Mizukami, M.; Moteki, M.; Kurihara, K. Hydrogen-Bonded Macrocluster Formation of Ethanol on Silica Surfaces in Cyclohexane1. *J. Am. Chem. Soc.* **2002**, *124*, 12889−12897.

(23) Zhuang, X. W.; Miranda, P. B.; Kim, D.; Shen, Y. R. Mapping Molecular Orientation and Conformation at Interfaces by Surface Nonlinear Optics. *Phys. Rev. B* **1999**, *59*, 12632−12640.

(24) Wei, X.; Hong, S. C.; Zhuang, X. W.; Goto, T.; Shen, Y. R. Nonlinear Optical Studies of Liquid Crystal Alignment on a Rubbed Polyvinyl Alcohol Surface. *Phys. Rev. E* **2000**, *62*, 5160−5172.

(25) Shen, Y. R. Surfaces Probed by Nonlinear Optics. *Surf. Sci.* **1994**, *299*, 551−562.

(26) Du, Q.; Freysz, E.; Shen, Y. R. Vibrational-Spectra of Water-Molecules at Quartz Water Interfaces. *Phys. Rev. Lett.* **1994**, *72*, 238−241.

(27) Richmond, G. L. Molecular Bonding and Interactions at Aqueous Surfaces As Probed by Vibrational Sum Frequency Spectroscopy. *Chem. Rev.* **2002**, *102*, 2693−2724.

(28) Shultz, M. J.; Schnitzer, C.; Simonelli, D.; Baldelli, S. Sum Frequency Generation Spectroscopy of the Aqueous Interface: Ionic and Soluble Molecular Solutions. *Int. Rev. Phys. Chem.* **2000**, *19*, 123−153.

(29) Eisenthal, K. B. Liquid Interfaces Probed by Second-Harmonic and Sum-Frequency Spectroscopy. *Chem. Rev.* **1996**, *96*, 1343−1360.

(30) Brown, M. G.; Raymond, E. A.; Allen, H. C.; Scatena, L. F.; Richmond, G. L. The Analysis of Interference Effects in the Sum Frequency Spectra of Water Interfaces. *J. Phys. Chem. A* **2000**, *104*, 10220−10226.

(31) Zhang, L. N.; Liu, W. T.; Shen, Y. R.; Cahill, D. G. Competitive Molecular Adsorption at Liquid/Solid Interfaces: A Study by Sum-Frequency Vibrational Spectroscopy. *J. Phys. Chem. C* **2007**, *111*, 2069−2076.

(32) Liu, W. T.; Zhang, L. N.; Shen, Y. R. Interfacial Layer Structure at Alcohol/Silica Interfaces Probed by Sum-Frequency Vibrational Spectroscopy. *Chem. Phys. Lett.* **2005**, *412*, 206−209.

(33) Miranda, P. B.; Shen, Y. R. Liquid Interfaces: A Study by Sum-Frequency Vibrational Spectroscopy. *J. Phys. Chem. B* **1999**, *103*, 3292−3307.

(34) Chen, Z.; Shen, Y. R.; Somorjai, G. A. Studies of Polymer Surfaces by Sum Frequency Generation Vibrational Spectroscopy. *Annu. Rev. Phys. Chem.* **2002**, *53*, 437−465.

(35) Shultz, M. J.; Baldelli, S.; Schnitzer, C.; Simonelli, D. Aqueous Solution/Air Interfaces Probed with Sum Frequency Generation Spectroscopy. *J. Phys. Chem. B* **2002**, *106*, 5313−5324.

(36) Gan, W.; Zhang, Z.; Feng, R. R.; Wang, H. F. Spectral Interference and Molecular Conformation at Liquid Interface with Sum Frequency Generation Vibrational Spectroscopy (SFG-VS). *J. Phys. Chem. C* **2007**, *111*, 8726−8738.

(37) Wang, H. F.; Gan, W.; Lu, R.; Rao, Y.; Wu, B. H. Quantitative Spectral and Orientational Analysis in Surface Sum Frequency Generation Vibrational Spectroscopy (SFG-VS). *Int. Rev. Phys. Chem.* **2005**, *24*, 191−256.

(38) Wang, C. Y.; Groenzin, H.; Shultz, M. J. Surface Characterization of Nanoscale TiO_2 Film by Sum Frequency Generation Using Methanol As a Molecular Probe. *J. Phys. Chem. B* **2004**, *108*, 265−272.

(39) Adamson, A. G., Gast, A. P. *Physical Chemistry of Surfaces*, 6th ed.; Wiley and Sons: New York, 1997; pp 605, 611.

(40) Fan, H. F.; Li, F. P.; Zare, R. N.; Lin, K. C. Characterization of Two Types of Silanol Groups on Fused-Silica Surfaces Using

DOI: 10.1021/jp510706u
J. Phys. Chem. A 2015, 119, 4573−4580

Evanescent-Wave Cavity Ring-down Spectroscopy. *Anal. Chem.* **2007**, *79*, 3654−3661.
(41) Shen, Y. R. Phase-Sensitive Sum-Frequency Spectroscopy. *Annu. Rev. Phys. Chem.* **2013**, *64*, 129−150.
(42) Ji, N.; Ostroverkhov, V.; Tian, C. S.; Shen, Y. R. Characterization of Vibrational Resonances of Water-Vapor Interfaces by Phase-Sensitive Sum-Frequency Spectroscopy. *Phys. Rev. Lett.* **2008**, *100*, 096102.
(43) Tian, C. S.; Shen, Y. R. Structure and Charging of Hydrophobic Material/Water Interfaces Studied by Phase-Sensitive Sum-Frequency Vibrational Spectroscopy. *Proc. Natl. Acad. Sci. U. S. A.* **2009**, *106*, 15148−15153.
(44) Tian, C. S.; Byrnes, S. J.; Han, H. L.; Shen, Y. R. Surface Propensities of Atmospherically Relevant Ions in Salt Solutions Revealed by Phase-Sensitive Sum Frequency Vibrational Spectroscopy. *J. Phys. Chem. Lett.* **2011**, *2*, 1946−1949.
(45) Yu, Y. Q.; Lin, K.; Zhou, X. G.; Wang, H.; Liu, S. L.; Ma, X. X. New C-H Stretching Vibrational Spectral Features in the Raman Spectra of Gaseous and Liquid Ethanol. *J. Phys. Chem. C* **2007**, *111*, 8971−8978.
(46) Nihonyanagi, S.; Yamaguchi, S.; Tahara, T. Direct Evidence for Orientational Flip-Flop of Water Molecules at Charged Interfaces: A Heterodyne-Detected Vibrational Sum Frequency Generation Study. *J. Chem. Phys.* **2009**, *130*, 204704.
(47) Bell, G. R.; Bain, C. D.; Ward, R. N. Sum-Frequency Vibrational Spectroscopy of Soluble Surfactants at the Air/Water Interface. *J. Chem. Soc., Faraday Trans.* **1996**, *92*, 515−523.
(48) Wolfrum, K.; Laubereau, A. Vibrational Sum-Frequency Spectroscopy of an Adsorbed Monolayer of Hexadecanol on Water - Destructive Interference of Adjacent Lines. *Chem. Phys. Lett.* **1994**, *228*, 83−88.
(49) Zhang, D.; Gutow, J.; Eisenthal, K. B. Vibrational-Spectra, Orientations, and Phase-Transitions in Long-Chain Amphiphiles at the Air-Water-Interface - Probing the Head and Tail Groups by Sum-Frequency Generation. *J. Phys. Chem.* **1994**, *98*, 13729−13734.
(50) Usenko, A. S. Competitive Adsorption of a Two-Component Gas on a Deformable Adsorbent. *Phys. Scr.* **2014**, *89*, 065701.

DOI: 10.1021/jp510706u
J. Phys. Chem. A 2015, 119, 4573−4580